

A Puzzle Involving Galactic Bulge Microlensing Events ¹

Judith G. Cohen², Andrew Gould³, Ian B. Thompson⁴, Sofia Feltzing⁵, Thomas Bensby⁶,
Jennifer A. Johnson³, Wenjin Huang⁷, Jorge Meléndez⁸, Sara Lucatello⁹ & Martin
Asplund¹⁰

ABSTRACT

We study a sample of 16 microlensed Galactic bulge main sequence turnoff region stars for which high dispersion spectra have been obtained with detailed abundance analyses. We demonstrate that there is a very strong and highly statistically significant correlation between the maximum magnification of the microlensed bulge star and the value of the [Fe/H] deduced from the high resolution spectrum of each object. Physics demands that this correlation, assuming it to be real, be the result of some sample bias. We suggest several possible

¹Based in part on observations obtained at the W.M. Keck Observatory, which is operated jointly by the California Institute of Technology, the University of California, and the National Aeronautics and Space Administration.

²Palomar Observatory, Mail Stop 249-17, California Institute of Technology, Pasadena, Ca., 91125, jlc@astro.caltech.edu

³Department of Astronomy, Ohio State University, 140 W. 18th Ave., Columbus, OH 43210; gould,jaj@astronomy.ohio-state.edu

⁴Carnegie Observatories, 813 Santa Barbara Street, Pasadena, Ca. 91101, ian@obs.carnegiescience.edu

⁴Lund Observatory, Box 43, SE-22100 Lund, Sweden, sofia@astro.lu.se

⁶European Southern Observatory, Alonso de Cordova 3107, Vitacura, Casilla 19001, Santiago 19, Chile, tbensby@eso.org

⁷Palomar Observatory, Mail Stop 105-24, California Institute of Technology, Pasadena, Ca., 91125, current address: University of Washington, Department of Astronomy, Box 351580, Seattle, Washington, 98195-1580, hwenjin@astro.washington.edu

⁸Centro de Astrofísica da Universidade do Porto, Rua das Estrelas, 4150-762 Porto, Portugal (jorge@astro.up.pt)

⁹INAF-Astronomical Observatory of Padova, Vicolo dell'Osservatorio 5, 35122 Padova, Italy, and Excellence Cluster Universe, Technische Universität München, Boltzmannstr. 2 D-85748 Garching, Germany, sara.lucatello@oapd.inaf.it

¹⁰Max Planck Institute for Astrophysics, Postfach 1317, 85741 Garching, Germany, asplund@MPA-Garching.MPG.DE

explanations, but are forced to reject them all, and are left puzzled. To obtain a reliable metallicity distribution in the Galactic bulge based on microlensed dwarf stars it will be necessary to resolve this issue through the course of additional observations.

Subject headings: gravitational lensing — stars: abundances — Galaxy: bulge

1. Introduction

Microlensing occurs when a “lens” (star, planet, black hole, etc) becomes closely aligned with a more distant “source” star, whose image it both magnifies and distorts. Microlensing of stars in the Galactic bulge offers the possibility of studying in detail stars that are too faint for such even with the largest existing telescopes without a microlensing boost. The lens is usually a star the Galactic bulge, but sometimes in the disk of the Milky Way (Dominik 2006).

Bulge giants are bright enough that high-dispersion spectra can routinely be obtained with 8 m class telescopes. Extensive surveys of such giants at optical wavelengths (see, e.g. Fulbright, McWilliam & Rich 2006) have been carried out to construct the metallicity distribution function (MDF) for the bulge, many of them in Baade’s Window ($b \sim -4^\circ$), the innermost field of relatively low reddening. Zoccali et al. (2008) have presented results of a survey of $[\text{Fe}/\text{H}]$ in the Galactic bulge from spectra of about 800 stars with $\lambda/\Delta\lambda = 20,000$. They find a radial gradient in $[\text{Fe}/\text{H}]$ within the bulge with the mean value going from $+0.03$ dex at $b = -4^\circ$ to -0.12 dex at $b = -6^\circ$, and a sharp cutoff toward higher metallicities with less than 5% of the sample in Baade’s Window having $[\text{Fe}/\text{H}] > 0.4$ dex. Rich, Origlia & Valenti (2007), who reach into $(l, b) = (0^\circ, -1^\circ)$ with high dispersion in the near-IR, still find a sub-solar mean metallicity of -0.22 ± 0.01 dex.

The ability to obtain high resolution, high quality spectra of microlensed Galactic bulge dwarfs and to carry out a detailed abundance analysis offers an independent apparently unbiased way to determine the MDF of Galactic bulge stars, as well as their detailed chemical inventory. In principle the abundance analysis of an upper main sequence dwarf is much easier and less prone to error for spectra of a fixed signal-to-noise ratio than that of a much cooler but much brighter bulge giant with a very complex spectrum full of blends and strong molecular bands.

2. The Sample of Microlensed Galactic Bulge Stars

We consider here the sample of subgiants near the main sequence turnoff (MSTO), stars at the MSTO, or dwarfs of slightly lower luminosity than the MSTO which have had high-magnification microlensing events during which high-dispersion spectra have been obtained with large optical telescopes. We denote this group as the microlensed MSTO dwarfs in the Galactic bulge. Our sample includes all such stars with published abundance analyses.

The pioneering work of Cavallo et al. (2003) includes three such stars, MACHO-98-BLG-6, MACHO-99-BLG-1¹, and MACHO-99-BLG22; see, e.g. Stubbs et al (1993) and Alcock et al (1999) for descriptions of the MACHO survey. Johnson et al. (2007) (MOA-2006-BLG265) were the first to piggy-back on the microlensing planet hunters, who prize high-magnification events because of their extreme sensitivity to planets (Udalski et al. 2005; Gould et al. 2006; Gaudi et al. 2008). This star proved to be extremely metal-rich, much more so than the bulk of the much larger samples of bulge giants, arousing considerable interest. Improvements in the current generation of microlensing surveys of the bulge, the OGLE collaboration² (Udalski 2003) and the MOA collaboration³ (Bond et al 2002), led to increasing numbers of alerts; they together find a total of about 800 microlensing events per year, of which the Microlensing Follow Up Network (μ FUN)⁴ is able to identify about 10 as high-magnification events.

Recognition of the importance of observations of transient sources has led to modifications in telescope operations to enhance our ability to take advantage of such brief opportunities. Thus Johnson et al. (2008) (MOA-2006-BLG99) and Cohen et al. (2008) (OGLE-2007-BLG-349S), the latter spectrum with signal-to-noise ratio/spectral resolution element (SNR) > 90 for $\lambda > 5500 \text{ \AA}$, rapidly followed, as did Cohen et al. (2009) (MOA-2008-BLG-310S and 311S), as well as the very recently completed analysis of OGLE-2007-BLG514S (Epstein et al. 2010). Each of these microlensed MSTO bulge stars turned out to have very high [Fe/H]. The first three of these led to the suggestion by Cohen et al. (2008) that the true MDF in the Galactic bulge was that of the dwarfs, characterized by significantly higher mean [Fe/H] than that of the giant bulge samples.

All of these stars were observed with either HIRES (Vogt et al. 1994) at the Keck I telescope or the MIKE spectrograph (Bernstein et al. 2003) at the 6.5 m Magellan Clay Telescope

¹We omit this star as it's spectrum shows double lines according to Bensby et al. (2010).

²<http://www.astrouw.edu.pl/~ogle/ogle3/ews/ews.html>

³<http://www.phys.canterbury.ac.nz/moa>

⁴<http://www.astronomy.ohio-state.edu/~microfun/>

at the Las Campanas Observatory. Last year, a group led by S. Feltzing, T. Bensby and J. Johnson began observing MSTO microlensed bulge stars with UVES (Dekker et al. 2000) at the VLT. Results from two stars, OGLE-2008-BLG-209S (Bensby et al. 2009a, a MIKE spectrum) and OGLE-2009-BLG-076S (Bensby et al. 2009b) followed, both of which were metal-poor, with $[\text{Fe}/\text{H}]$ -0.33 and -0.76 dex respectively. Bensby et al. (2010) suggested that the previous high metallicities for microlensed bulge dwarfs might be just a matter of chance; they find that they cannot reject the possibility that the MDFs for the bulge giants and microlensed dwarfs are identical.

Here we adopt the $[\text{Fe}/\text{H}]$ and their associated uncertainties given in the published papers referenced above. To this sample we add MOA-2009-BLG259S, observed with HIRES/Keck in July 2009 for which Cohen et al. (in preparation) find $[\text{Fe}/\text{H}] = +0.55 \pm 0.10$ dex. We also add five microlensed bulge dwarfs observed with the VLT from Bensby et al. (2010) for a total sample of 16 microlensed MSTO Galactic bulge stars.

3. The Maximum Magnification of the Microlensing Events

The maximum magnification, $A(max)$, of each of these microlensing events is based for all recent events on fits to high cadence photometry obtained by μFUN ⁵. Poindexter et al. (2005) give $A(max)$ for the MACHO events; we use Janczak et al (2009) for MOA-2008-BLG-310S. $A(max)$, the ratio of the apparent brightness at the peak of the microlensing event to that before or after, is independent of reddening. It ranges from 5 to ~ 1000 for our sample stars (see Table 1). Figure 1 shows the relationship between $A(max)$ for the event and the $[\text{Fe}/\text{H}]$ of the source derived from the high-dispersion spectra for each of the 16 microlensed Galactic bulge stars in our sample.

It is apparent from Figure 1 that there is a very strong correlation between $A(max)$ and $[\text{Fe}/\text{H}]$ for the MSTO sample of microlensed bulge stars. A similarly strong correlation is shown when A at the time the spectra were acquired is used instead. A Spearman rank test indicates that the two-sided probability that $A(max)$ is not correlated with $[\text{Fe}/\text{H}]$ is 5×10^{-3} . If MACHO-1998-BLG6, which Bensby et al. (2010) consider a low luminosity giant, not a subgiant, is omitted, the two-sided probability for the remaining 15 stars becomes 6×10^{-3} , not significantly larger. While in principle this could be a statistical fluke, the formal probability of this is sufficiently low to investigate the implications of it being a real effect.

⁵The $A(max)$ from the MOA web site are preliminary values only.

Figure 2 shows the locations on the sky of the sample of microlensed bulge stars. The region of positive Galactic latitude in general has significantly larger extinction than that of negative b in the region of the Galactic center, and much of that area is not covered by any microlensing survey. There is no obvious difference in the projected spatial distribution on the sky of the very high vs the lower $A(max)$ bulge microlensed MSTO stars. The maximum projected distance from the Galactic center for a star in our sample is 6.6° (0.9 kpc), the minimum 2.2° ; the median is 4.0° , the same as that of Baade’s Window.

Thus in addition to the discrepancy between the MDF of the bulge giants vs that of the microlensed dwarfs reviewed in §1, an even more puzzling and potentially more serious problem is introduced by Fig. 1. At first glance this figure suggests the presence of two populations, one at $[Fe/H]$ about $+0.35$ dex with $\sigma([Fe/H])$ small and with $A(max) > 200$, and one with mean $[Fe/H]$ considerably lower at about -0.4 dex, a larger dispersion in metallicity, and with $A(max) < 200$. Since we have already shown that the projected distributions of the low and high magnification events are similar, we next consider systematically different positions along the line of sight. One might imagine that spatially separating the high and low metallicity microlensing events, having them arise in regions of different stellar density (presumably closer or further from the Galactic center) in the presence of radial gradients in $[Fe/H]$ within the bulge (already established as present further out in the bulge by Zoccali et al. 2008) could lead to the very strong correlation seen in Figure 1.

Microlensing with stars as both sources and as lenses is a phenomenon depending only on geometry (i.e. distances and impact parameter) and the mass of the lens. An ensemble of microlensing events also has properties that depend on the spatial density of the sources and lenses. The distribution in magnification for a particular source and a particular lens always has a much higher probability for events with large impact parameter (low $A(max)$) than it does for events with small impact parameter (high-magnification events). The absence of any event with high $[Fe/H]$ and $A(max) < 200$ given the many very high $A(max)$, high $[Fe/H]$ events we see poses an insurmountable problem to any hypothesis that seeks to explain the trend seen in Fig. 1 through a mechanism of spatially separate populations within the bulge with differing mean metallicities, densities, etc.

If the basic physical laws governing microlensing are not to be violated, there must be a previously unrecognized sample bias that produces the strong correlation between $A(max)$ and $[Fe/H]$ seen in Fig. 1. We consider several possibilities below.

(1) When the angular size of the impact parameter for the microlensing event is so small that it becomes comparable to the angular size of the source star’s radius, finite source effects, i.e. differential magnification of the limb relative to that of the center of the disk of the source star, become important. This occurs only in very high $A(max)$ events, and

affects the strength of spectral lines, which could potentially produce a spurious $[\text{Fe}/\text{H}]$ in the highest $A(\text{max})$ events, leading to a systematic sample bias. Johnson, Dong & Gould (2010) carried out detailed abundance studies of synthetic spectra of highly magnified dwarf stars. They concluded that the effects are always less than 0.05 dex, which is much too small to account for the effect seen in Fig. 1.

(2) Perhaps in the very crowded fields of the Galactic bulge, the spectra in low magnification events include a substantial contribution from close neighbors of the microlensed dwarf, while when $A(\text{max})$ is large, spectroscopic observations only detect the source star. We have evaluated the contribution of blending stars by comparing the unlensed brightness inferred from the microlensing light curve with that from OGLE or MOA images long before the event⁶. In the worst case (MOA-2009-BLG493), there is a 10% contribution at the time of observation, the second worst case has a 5% contribution by blending stars; for all other events this is not an issue. This demonstrates that blending is not the answer. Furthermore double-lined spectra are not seen among any of these microlensed dwarfs.

(3) Perhaps for some of the events the source is a foreground disk star. If disk stars have a lower mean $[\text{Fe}/\text{H}]$ than that of the bulge and if such events preferentially include those with low $A(\text{max})$, this could reproduce the observed relationship shown in Fig. 1. However, extrapolating the linear fit to the metallicity gradient determined by Luck, Kovtyukh & Andrievsky (2006) outside 4 kpc from the center further inward, the disk would reach $[\text{Fe}/\text{H}] +0.5$ dex at $R_{GC} = 1$ kpc. In addition, calculations of the probability of microlensing for a source in the Galactic disk (see e.g. Kane & Sahu 2006) demonstrate that the source of a microlensing event towards the bulge actually be a foreground disk star is unlikely. Furthermore the measured radial velocities show that the sources of these microlensing events are a kinematically hot population with $\sigma(v_r)$ much too large for the Galactic disk; see Fig. 2. Additional arguments supporting a bulge origin for the MSTO microlensing dwarfs can be found in e.g. Bensby et al. (2010).

(4) Perhaps the fault lies in systematic errors in $[\text{Fe}/\text{H}]$. There is a real sampling bias among the active groups working in this area. The initial results of the analyses of two microlensed MSTO bulge stars by Johnson et al. (2007, 2008) yielded surprisingly high metallicities. Even Solar type dwarfs with such high $[\text{Fe}/\text{H}]$ have complex spectra, with many blended and overlapping features, and the photometry is not trustworthy in regions with such high and variable reddening. Cohen and Thompson, who lead the efforts at the Keck and Magellan Observatories, believed that such a controversial issue could only be finally settled on the basis of very high signal-to-noise spectra. This meant that they triggered

⁶The required data are not easily available for the MACHO events.

target-of-opportunity observations only for the brightest of the microlensed bulge dwarfs, which tend to be those with the highest $A(max)$. The VLT group has observed events with a larger range of brightness, and hence of $A(max)$.

In light of the sample bias between the VLT and the Magellan/Keck groups, the relevant question is whether the $[Fe/H]$ values determined by the various groups involved are on a consistent scale. Since the low magnification events are in general fainter, one might expect the resulting spectra to be on average of lower quality with lower signal-to-noise ratios. Given that line crowding and blending make the definition of the continuum in these spectra difficult, this might produce a bias of underestimating $[Fe/H]$ in the required sense.

Bensby et al. (2009a) and Bensby et al. (2010) present comparisons of multiple independent analyses by J. Johnson, J. G. Cohen and T. Bensby, and collaborators of HIRES or Mike spectra of six microlensed MSTO stars included in our sample. The deduced $[Fe/H]$ values are identical to within ± 0.10 dex in all cases. Very recently, the two lowest SNR spectrum from the VLT sample, OGLE-2009-BLG-076S and MOA-2009-BLG-475, were also analyzed by J. Cohen, and even for these very low SNR spectra the derived $[Fe/H]$ values were in agreement to within the uncertainties, for the former being -0.45 ± 0.20 vs. -0.72 ± 0.12 dex and for the latter -0.49 ± 0.20 vs -0.54 ± 0.17 dex.

We thus have established that there is good agreement in the derived $[Fe/H]$ from detailed abundance analyses when the three groups independently analyze the same spectrum of a microlensed MSTO bulge star. The remaining issue is whether $[Fe/H]$ derived from a spectrum of a microlensed MSTO bulge dwarf is independent of the SNR within the range encompassed by our sample of 16 microlensed bulge MSTO stars. T. Bensby has carried out a test on the high SNR Keck spectrum of OGLE-2007-BLG349, degrading it to SNR ~ 30 , and finds that the deduced $[Fe/H]$ changes by less than 0.05 dex. We emphasize that errors in $[Fe/H]$ arising from different analyses or from the SNR of the observations appear to be too small to be the origin of the strong correlation between $A(max)$ and $[Fe/H]$ seen in Fig. 1.

(5) There are some biases in the detectability of a microlensing event that depend on metallicity. These arise because the unlensed luminosity of a dwarf of a given mass and age is a function of metallicity. Tests with the Y^2 isochrones (Yi et al. 2003) show that for a fixed age (we adopt 10 Gyr), the mass of a star at the turnoff is higher as metallicity increases and the turnoff becomes somewhat fainter in M_I . We adopt a Salpeter IMF, and compare two populations with this age and with $[Fe/H]$ between -0.9 and $+0.6$ dex. While for a population with a fixed total mass, the total number of stars is significantly different in the two cases, the ratio of the the number of stars on the upper RGB selected in a fixed range of M_I to the number of stars in the turnoff region is approximately constant. Hence this

cannot explain differences in the MDF between the bulge giants and the bulge microlensed MSTO dwarfs nor lead to the correlation between $A(max)$ and $[Fe/H]$ seen in Fig. 1.

(6) Perhaps the procedures by which microlensing events are identified by the large surveys are biased in some way. This has been checked by A. Gould, who went through the entire set of OGLE microlensing alerts from 2008, examining each event, eliminating binaries, and redetermining $A(max)$ using all available photometry when necessary. He found that the number of microlensing alerts as a function of $A(max)$, equivalent to $1/u_0$ for $A(max) > 4$, has the form expected for selection of a sample unbiased in $A(max)$. Fig. 3 shows the result, namely there is a linear relationship between cumulative counts and u_0 for $A(max) > 15$. This is the expected relation for uniform completeness in the OGLE microlensing survey over each of the three ranges of unlensed source magnitude considered. The inset shows that the total number of events for $A(max) > 15$ in each bin increases for fainter source stars, as expected, but this is because there are more faint stars than bright ones. Very high magnification events are very rare. A table of updated $A(max)$ for the accepted 2008 OGLE events is available as Table 2 (on-line version only).

While we believe that the source of the very strong correlation seen in Figure 1 is some bias in the sample of microlensed bulge MSTO dwarfs, we have been unable to identify the source of the bias. Every mechanism that we have thought of can be ruled out with varying degrees of certainty. Unfortunately, until the sample bias for the microlensed MSTO bulge dwarfs is identified, the derived bulge-dwarf MDF and its comparison to the bulge-giant MDF must be treated very cautiously.

Although suitable high-magnification events are rare and lining up the necessary instruments/telescopes/clear weather at just the right time is difficult, with the Keck, Magellan, and VLT observatories all quite interested in this problem, the samples of MSTO bulge microlensed dwarfs with high-dispersion spectra has risen rapidly, and will continue to do so. But, assuming that the correlation between $A(max)$ of the event and $[Fe/H]$ of the source star continues to hold as the sample increases, what is really needed now just as urgently as larger samples is a new insight into what is causing the very strong correlation we have found between the maximum magnification of a microlensing event for bulge MSTO stars and their metallicities shown in Fig. 1.

We are grateful to the many people who have worked to make the Keck Telescope and HIRES a reality and to operate and maintain the Keck Observatory. The authors wish to extend special thanks to those of Hawaiian ancestry on whose sacred mountain we are privileged to be guests. Without their generous hospitality, none of the observations presented herein would have been possible. We thank Chris Hirata and Sterl Phinney for

helpful discussions. J.G.C. thanks NSF grants AST-0507219 and AST-0908139 for partial support. Work by A.G. was supported by NSF grant AST-0757888. I.B.T. thanks NSF grant AST-0507325 for support.

REFERENCES

- Alcock, C. et al, PASP, 111, 1539
- Bensby, T. et al, 2009a, A&A, 499, 737
- Bensby, T. et al, 2009b, ApJ, 699, L174
- Bensby, T. et al, 2010, A&A, submitted (arXiv:0911.5076)
- Bernstein, R., Shtetman, S. A., Gunnels, S. M., Mochacki, S. & Athey, A. E., 2003, in *Instrument Design and Performance for Optical/Infrared Ground-Based Telescopes*, ed. I. Masanori & A. Moorhead, Proceedings of the SPIE, 4841, 1694
- Bond, I. et al, 2002, MNRAS, 333, 71
- Cavallo, R. M., Cook, K. H., Minniti, D. & Vandehei, T., 2003, SPIE, 4834, 66
- Cohen, J. G., Huang, W. J., Udalski, A., Gould, A. & Johnson, J. A., 2008, ApJ, 682, 1029
- Cohen, J. G. et al, 2009, ApJ, 699, 66
- Dekker, H. et al, 2000, SPIE, 4008, 53
- Dominik, M., 2006, MNRAS, 367, 669
- Epstein, C. R., Johnson, J. A., Dong, S., Udalski, A., Gould, A. & Becker, G., 2010, ApJ, submitted
- Fulbright, J. P., McWilliam, A. & Rich, R. M., 2006, ApJ, 636, 821
- Gaudi, B. S., et al. 2008, Science, 315, 927
- Gould, A., et al. 2006, ApJ, 644, L37
- Janczak, J. et al, 2009, ApJ, submitted (see Astro-ph/0908.0529)
- Johnson, J. A., Gal-Yam, A., Leonard, D. C., Simon, J. D., Udalski, A. & Gould, A., 2007, ApJ, 655, L3
- Johnson, J. A., Gaido, B.S., Sumi, T., Bond, I. A. & Gould, A., 2008, ApJ, , 685, 508
- Johnson, J. A., Dong, S. & Gould, A., 2010, ApJ, submitted (Astro-ph/0910.3670)
- Kane, S. R. & Sahu, K. C., 2006, ApJ, 637, 752

- Luck, R. E., Kovtyukh, V. V. & Andrievsky, S. M., 2006, *AJ*, 132, 902
- Poindexter, S., Afonso, C., Bennett, D. P., Glicenstein, J.-F., Gould, A. & Szymanski, M. K., 2005, *ApJ*, 633, 914
- Ramírez, S. V., Stephens, A., Frogel, J. A. & DePoy, D. L., 2000, *AJ*, 120, 833
- Rich, R. M., Origlia, L. & Valenti, E., 2007, *ApJ*, 665, L19
- Stubbs, C. W. et al, 1993, in *Proceedings of the SPIE, “Charge Coupled Devices and Solid State Optical Sensors III’*, ed. M. Blouke, 1900, 192
- Udalski, A. 2003, *Acta Astron.*, 53, 291
- Udalski, A., et al. 2005, *ApJ*, 628, L109
- Vogt, S. E. et al. 1994, *SPIE*, 2198, 362
- Yi, S., Kim, Y.-C., Demarque, P. & Alexander, D. R., 2003, *ApJS*, 143, 499
- Zocalli, M., Hill, V., Lecureur, A., Barbuy, B., Renzini, A., Minitti, D., Gomez, A. & Ortolani, S., 2008, *A&A*, 486, 177

Table 1. Data for Microlensed MSTO Bulge Stars

Name	Obs. Code ^a	$A(max)$	$A(obs)$ ^b	[Fe/H] ^c (dex)
MACHO-1998-BLG-6	K	5	4	−0.22
MACHO-1999-BLG22	K	28	12	−0.35
MOA-2006-BLG99	M	515	110	+0.36
OGLE-2006-BLG265S	K	210	135	+0.56
OGLE-2007-BLG349S	K	450	400	+0.56
OGLE-2007-BLG514S	M	1000	500	+0.33
OGLE-2008-BLG209	M	30	22	−0.33
MOA-2008-BLG-311	M	285	200	+0.26
MOA-2008-BLG-310S	M	380	313	+0.42
MOA-2009-BLG259	K	223	223	+0.55
OGLE-2009-BLG-076S	V	68	48	−0.76
MOA-2009-BLG-493	V	150	123	−0.71
MOA-2009-BLG-133	V	74	35	−0.67
MOA-2009-BLG-475	V	62	48	−0.54
MOA-2009-BLG-489	V	103	103	−0.18
MOA-2008-BLG-456	V	77	47	+0.12

^aM=Magellan, K=Keck, V=VLT.

^bMagnification at the time the spectroscopic observations were carried out.

^cReferences for each star are given in §2 of the text.

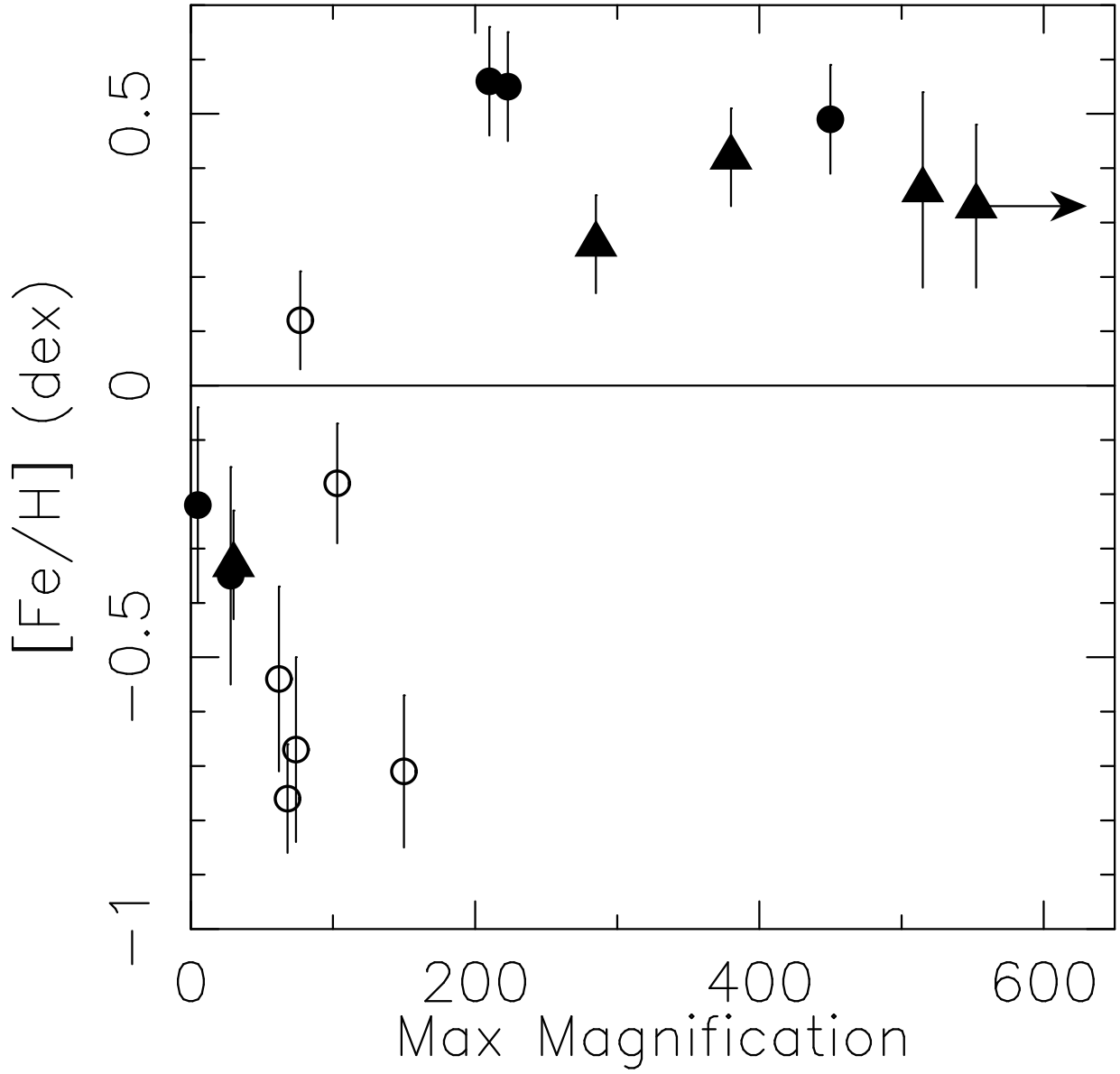


Fig. 1.— $[\text{Fe}/\text{H}]$ for the sample of 16 microlensed MSTO Galactic bulge stars with detailed abundance analyses is shown as a function of the maximum magnification achieved in each lensing event. Filled circles denote the Keck sample, filled triangles the Magellan sample, and open circles denote those with VLT spectra.

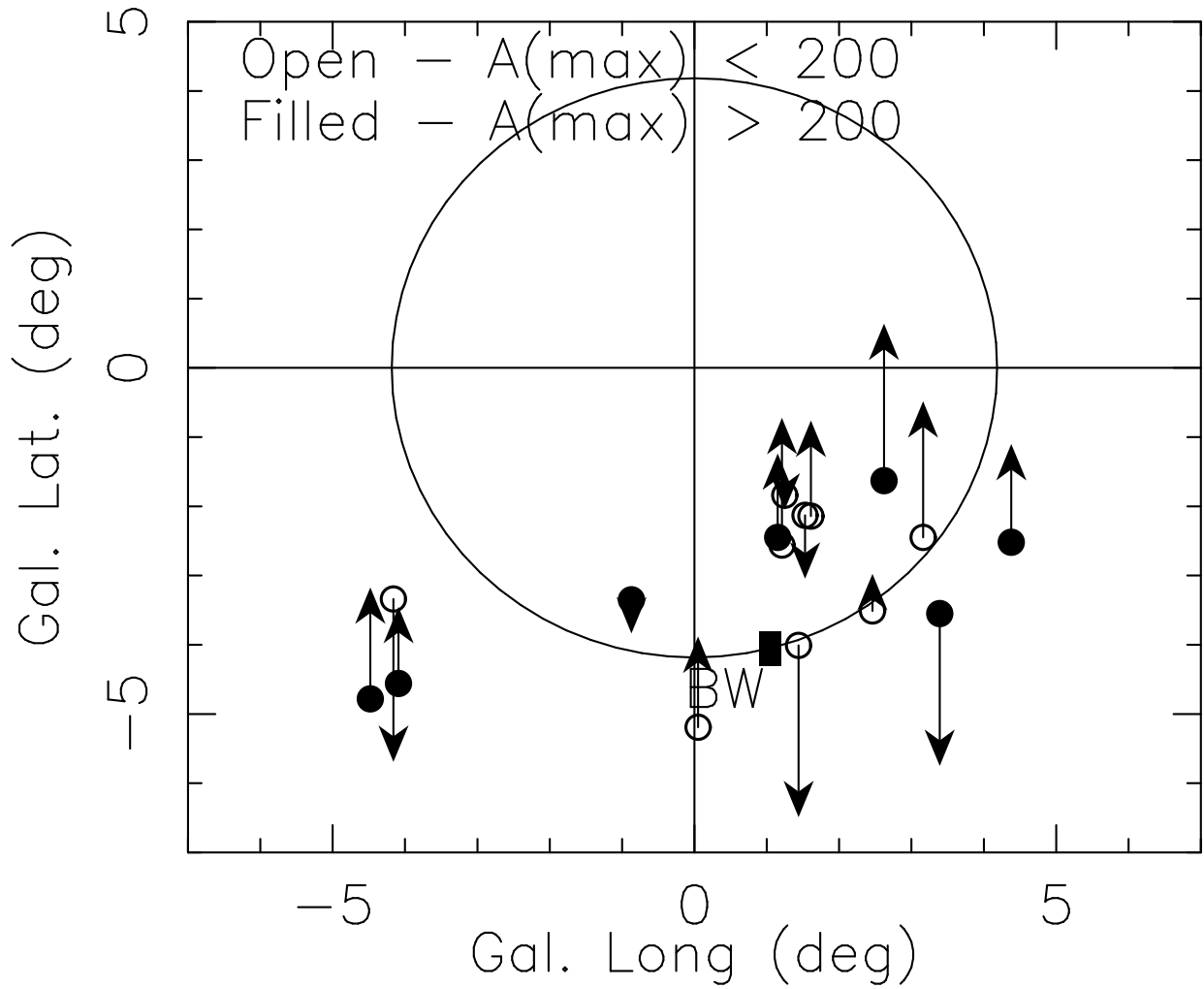


Fig. 2.— The distribution in Galactic latitude and longitude of the sample of 16 microlensed MSTO bulge stars. The heliocentric radial velocity for each star is indicated by an arrow, upward being positive, with a scale of 70 km s^{-1} per degree. Baade's Window is marked by the filled rectangle, and its Galactocentric radius is indicated by a circle.

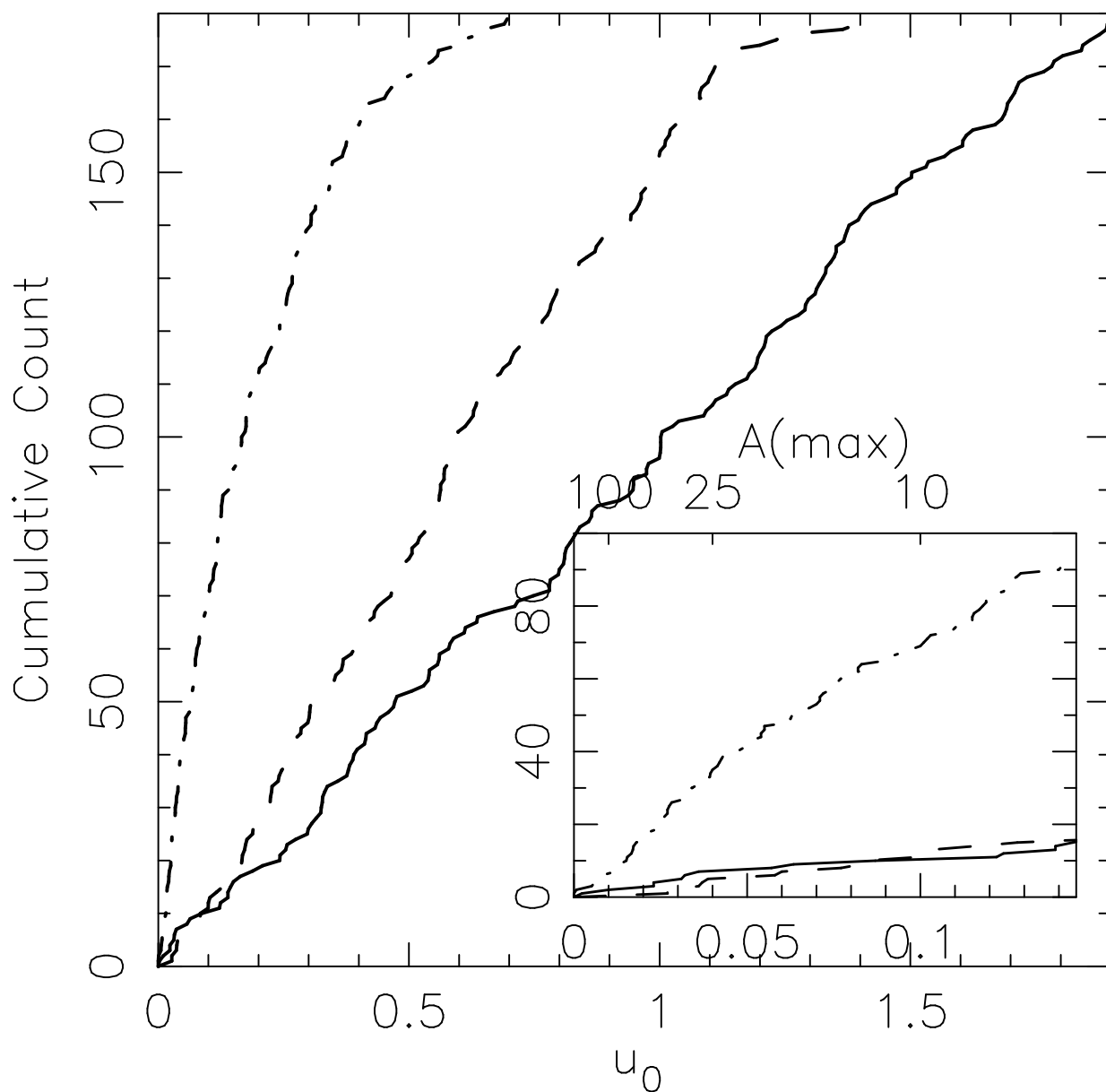


Fig. 3.— Cumulative counts of microlensing events as a function of u_0 (equivalent to $1/A(\max)$) for $A(\max) > 4$ for all OGLE alerts from 2008 that survived a check by hand for validity. Three different ranges of unlensed source brightness are shown - $I_s < 17.93$ (solid line), $17.93 < I_s < 19.28$ (dashed line), and $I_s > 19.28$ mag (dot-dashed line). (green line); bin boundaries were chosen so that 1/3 of the sample would be in each bin. For microlensing event selection by the OGLE survey to be independent of $A(\max)$, this relation should be a straight line, as is shown for high magnification events in the inset.

Table 2. Check of 2008 OGLE Bulge Microlensing Alerts

OGLE ID Number	u_0	t_E (days)	$I(source)$ (mag)	Code ^a
2	0.4110	16.767	17.187	1
3	0.0123	99.967	21.882	2
4	0.1500	17.761	16.574	2
5	0.5054	17.630	14.734	2
6	0.2840	71.667	19.505	2
9	0.7880	28.962	18.509	1
10	0.0830	72.709	19.536	1
11	0.2990	44.934	17.364	1
13	0.0230	74.357	16.206	1
14	0.3030	23.270	18.468	1
15	1.1050	6.526	17.918	1
16	0.3320	6.370	17.833	1
18	0.0100	14.982	16.334	2
20	0.4320	103.531	17.046	1
21	1.2130	38.661	17.829	1
22	0.3270	15.585	17.503	1
25	0.2850	22.929	18.947	1
27	0.3650	5.295	18.528	1
29	0.1000	7.337	19.880	1
31	0.0870	25.390	16.524	1
33	0.4360	37.001	17.445	1
35	0.9480	29.282	15.884	1
36	0.3970	18.174	19.535	1
37	0.7100	8.447	18.439	1
38	0.1570	87.566	19.175	1
40	0.4070	16.810	18.913	1
41	0.0580	37.042	18.920	1
42	0.1220	4.540	16.582	1
43	1.3480	3.928	15.990	1
44	0.2100	101.967	19.193	1

Table 2—Continued

OGLE ID Number	u_0	t_E (days)	$I(\text{source})$ (mag)	Code ^a
45	0.8220	50.960	18.069	1
46	0.1750	115.225	19.337	1
47	0.2460	16.650	18.774	1
48	1.1330	14.773	17.813	1
49	1.6040	15.167	17.244	1
51	0.3670	286.473	19.498	1
54	0.0330	19.922	20.143	1
55	0.0550	38.869	20.026	1
56	0.2260	5.897	19.876	1
57	0.0510	10.161	19.448	1
58	0.4170	21.195	18.144	1
60	0.0630	20.655	19.544	1
61	0.1400	9.846	19.648	1
62	0.1260	47.132	20.635	1
63	0.4150	4.387	17.731	1
64	0.9720	144.140	18.528	1
65	1.4220	16.517	17.925	1
66	1.7170	25.112	15.386	1
67	0.0270	20.003	18.791	1
68	1.6940	52.685	15.391	1
69	0.0760	17.980	19.946	1
70	0.0060	27.053	21.391	2
71	0.7630	18.618	18.617	1
72	1.0010	10.290	17.897	1
73	1.1110	5.969	18.058	1
75	0.5890	49.688	18.467	1
76	0.4650	31.204	19.301	1
77	0.0270	147.016	22.163	1
79	1.0610	20.639	18.298	1
80	1.2420	13.690	17.926	1

Table 2—Continued

OGLE ID Number	u_0	t_E (days)	$I(\text{source})$ (mag)	Code ^a
81	0.6350	95.013	15.726	1
82	0.5790	14.229	16.769	1
83	0.0720	38.008	19.412	1
85	1.2110	7.514	17.468	1
86	0.1570	194.801	21.005	1
87	0.6560	3.265	19.139	1
88	0.3160	58.643	19.253	1
89	0.7800	25.708	17.749	1
90	0.4050	72.430	19.414	1
91	1.5680	7.871	17.494	1
92	0.7800	55.243	15.473	1
93	0.5610	15.265	18.020	1
94	0.2260	17.178	18.951	1
95	1.6820	8.903	17.121	1
96	0.5400	107.578	16.450	1
97	1.7120	33.313	16.937	1
99	0.1150	13.272	20.036	1
100	0.6820	22.663	19.106	1
101	1.2900	23.423	17.163	1
102	0.2840	61.710	17.978	1
103	0.8000	0.697	16.217	1
104	1.1220	12.682	18.542	1
105	0.1500	22.945	19.896	1
106	0.6960	9.439	19.493	1
107	0.3420	7.741	19.530	1
108	0.1600	56.427	19.629	1
109	0.4750	10.866	19.204	1
111	0.2470	58.643	20.274	1
112	0.3050	91.007	20.017	1
113	0.7480	9.762	17.875	1

Table 2—Continued

OGLE ID Number	u_0	t_E (days)	$I(\text{source})$ (mag)	Code ^a
114	1.3780	46.867	15.620	1
115	0.1500	32.691	20.783	1
116	1.0120	11.245	18.656	1
119	0.9780	167.630	17.819	1
120	0.4140	12.877	19.063	1
121	0.7200	49.192	18.884	1
123	0.0540	13.470	19.735	1
124	0.6420	20.399	18.811	1
126	0.6690	47.280	17.575	1
127	1.4100	26.572	17.809	1
128	1.0020	2.715	16.535	1
129	0.1880	84.009	18.446	1
130	0.5380	9.191	18.077	1
131	1.3700	15.818	16.989	1
132	0.1950	44.134	19.356	1
133	1.1000	37.567	18.203	1
134	1.3740	9.102	17.591	1
135	1.7010	61.954	14.646	1
136	0.2420	19.137	19.966	1
137	0.3510	71.293	19.034	1
138	0.1770	33.162	19.249	1
139	0.3020	9.248	19.028	1
140	0.0340	23.394	20.301	1
141	0.3220	16.292	19.559	1
142	0.3300	7.647	18.429	1
145	0.5590	29.933	19.466	1
147	1.2320	12.584	18.135	1
148	0.9840	7.901	18.073	1
149	0.3060	5.383	17.085	1
150	0.2390	24.258	19.102	1

Table 2—Continued

OGLE ID Number	u_0	t_E (days)	$I(source)$ (mag)	Code ^a
151	0.3150	5.431	17.075	1
152	0.2730	26.361	20.249	1
153	0.8710	7.597	18.392	1
154	0.2720	52.374	18.985	1
155	0.0270	33.970	19.073	1
156	1.1740	28.587	17.191	1
158	0.4310	4.015	19.205	1
159	1.4490	38.588	17.171	1
160	0.7980	4.060	15.655	1
161	0.3690	137.506	18.680	1
162	1.1790	2.376	16.895	1
163	0.3760	4.904	17.284	1
164	0.8950	83.671	18.157	1
165	0.0770	39.656	20.601	1
166	0.0360	11.814	19.908	1
167	0.1160	17.843	19.092	1
168	0.5500	6.921	19.260	1
169	0.5460	7.926	19.496	1
170	0.3130	313.114	19.702	1
171	1.8910	20.235	13.839	1
172	0.5980	7.028	18.450	1
173	0.1660	21.493	19.432	1
174	1.5020	22.624	17.345	1
175	1.3960	20.018	17.363	1
176	0.4730	6.178	18.598	1
177	1.2240	2.778	17.785	1
178	0.9930	7.326	18.201	1
179	0.1410	69.365	21.101	1
180	0.2410	8.487	19.235	1
181	0.0490	6.601	19.966	1

Table 2—Continued

OGLE ID Number	u_0	t_E (days)	$I(source)$ (mag)	Code ^a
182	0.0740	41.873	21.941	1
183	0.2080	14.114	16.389	1
185	0.7930	15.389	18.693	1
186	0.5700	3.512	19.107	1
188	0.0211	5.937	20.664	2
189	1.6120	16.042	16.641	1
190	0.9630	19.551	19.163	1
192	1.1510	8.149	17.622	1
193	0.2670	12.110	19.587	1
194	0.1920	4.073	19.282	1
195	0.4690	14.563	17.944	1
196	0.0570	22.087	17.289	1
197	0.1870	44.324	19.589	1
198	0.1670	4.632	19.067	1
199	0.0230	10.404	15.057	1
200	0.8550	24.919	17.975	1
201	0.3900	3.219	17.071	1
202	1.4720	65.209	17.920	1
203	1.0960	18.264	18.430	1
204	0.8650	43.871	16.877	1
205	1.6050	15.662	15.658	1
206	0.2650	40.297	18.865	1
207	0.7670	19.599	18.317	1
208	0.0310	24.011	16.705	1
209	0.0320	19.549	17.784	1
212	1.7820	7.416	17.146	1
213	0.5630	13.076	19.167	1
214	0.7830	12.514	18.715	1
215	0.1000	6.557	18.738	1
216	0.3910	9.651	18.244	1

Table 2—Continued

OGLE ID Number	u_0	t_E (days)	$I(\text{source})$ (mag)	Code ^a
217	1.3250	11.488	17.207	1
218	0.0500	5.712	19.596	2
220	0.5060	7.355	19.123	1
221	0.1680	9.516	19.284	1
222	0.9380	36.721	17.381	1
223	0.2980	211.089	18.897	1
224	1.3520	10.586	16.633	1
225	0.2600	38.254	18.798	1
226	0.5710	5.230	18.671	1
227	0.5820	15.501	17.839	1
228	1.6920	38.576	16.314	1
229	0.1390	53.994	17.688	1
230	0.4940	9.895	19.605	1
231	0.0362	42.592	20.249	2
232	0.3440	8.637	19.594	1
234	0.8220	13.720	18.828	1
235	0.8210	2.963	17.781	1
236	0.0820	10.354	20.400	1
237	0.3740	23.082	19.372	1
238	1.0320	18.433	18.822	1
239	0.4300	9.869	18.761	1
240	1.1060	21.793	18.567	1
241	0.3700	7.739	19.461	1
242	0.5890	13.436	17.170	1
244	1.7660	20.325	15.383	1
245	0.0248	26.516	19.684	2
246	0.3040	3.266	19.557	1
247	1.8440	12.598	16.436	1
248	0.1780	47.129	20.620	1
249	0.1155	15.442	19.990	2

Table 2—Continued

OGLE ID Number	u_0	t_E (days)	$I(\text{source})$ (mag)	Code ^a
250	1.2500	19.123	18.087	1
251	0.7010	46.523	19.183	1
252	0.4660	29.285	18.558	1
253	0.8740	2.942	19.000	1
254	0.0910	7.832	20.195	1
255	0.9030	1.228	18.056	1
257	0.0250	7.324	20.053	2
260	0.0830	8.336	18.372	1
261	0.0392	14.408	20.876	2
262	1.0490	9.563	18.518	1
264	0.0180	8.020	22.635	2
265	0.8140	38.742	17.428	1
266	1.0010	10.392	18.410	1
267	0.9430	9.989	19.174	1
268	0.6380	34.913	18.706	1
269	1.9930	14.415	15.287	1
270	0.0120	100.000	19.990	2
271	0.2800	28.039	20.149	1
272	0.0051	57.868	22.189	2
273	1.2080	6.524	17.731	1
274	1.2760	3.591	17.772	1
275	0.0620	57.587	21.741	1
277	0.1250	4.072	19.532	1
278	0.5570	18.850	20.108	1
279	0.0007	96.480	20.794	2
280	0.2420	7.106	20.133	1
281	0.1740	2.818	19.197	1
282	1.8770	7.477	16.471	1
283	0.2000	23.756	20.451	1
284	0.0740	37.999	20.745	1

Table 2—Continued

OGLE ID Number	u_0	t_E (days)	$I(source)$ (mag)	Code ^a
285	0.2230	28.121	19.201	1
286	0.0340	36.494	19.611	1
287	0.4570	60.637	19.932	1
288	0.2560	8.024	19.364	1
289	0.9470	6.115	17.441	1
290	0.0023	16.226	16.908	2
291	0.8400	4.508	19.205	1
292	0.0322	3.335	20.367	2
293	0.1190	124.762	21.440	1
294	0.1660	140.097	19.906	1
295	0.9940	32.646	18.983	1
296	0.5780	5.492	19.024	1
297	0.5990	12.202	20.090	1
298	0.8890	7.782	18.940	1
299	0.0550	20.684	20.704	1
300	0.1100	22.513	20.416	1
301	0.1650	26.832	18.788	1
303	0.0220	35.902	19.684	2
304	0.4770	23.326	19.270	1
305	0.8410	2.272	17.537	1
306	0.3760	75.076	20.034	1
307	0.0387	4.074	19.264	2
308	0.0820	14.064	20.003	1
309	0.6360	7.583	19.172	1
310	0.3790	76.739	15.531	1
312	0.0540	32.006	19.816	1
313	0.3850	29.400	18.922	1
314	0.2680	45.988	20.380	1
315	1.4020	6.346	14.710	1
317	0.0700	7.056	19.506	1

Table 2—Continued

OGLE ID Number	u_0	t_E (days)	$I(source)$ (mag)	Code ^a
318	0.2540	50.081	15.990	1
319	1.1290	34.808	18.337	1
321	0.5170	0.362	17.947	1
322	0.5000	27.832	18.802	1
323	0.7170	8.564	15.119	1
324	0.6120	7.817	18.454	1
325	0.3580	25.658	17.552	1
326	0.3440	32.978	19.689	1
327	0.0081	14.947	21.326	1
328	1.2010	2.712	17.690	1
329	0.6200	7.339	18.284	1
331	0.4950	56.046	19.733	1
332	1.3950	18.521	18.186	1
333	0.0360	10.454	15.053	2
334	0.4060	8.784	19.444	1
335	0.1180	104.358	19.564	1
336	0.1010	53.246	19.859	1
338	0.6100	11.048	16.518	1
339	0.3370	24.972	16.578	1
340	0.1240	6.607	16.653	1
341	0.0680	24.094	20.857	1
343	0.0710	26.663	20.284	1
345	1.1960	13.160	16.763	1
346	0.0433	42.426	20.730	2
349	0.0282	24.366	19.572	2
350	0.2910	117.256	19.724	1
351	1.3310	3.618	16.700	1
352	0.2670	36.215	19.784	1
354	0.1450	87.932	21.174	1
356	1.2540	9.402	17.811	1

Table 2—Continued

OGLE ID Number	u_0	t_E (days)	$I(source)$ (mag)	Code ^a
357	0.9530	7.202	17.998	1
358	0.0151	63.449	22.228	2
359	0.0275	3.078	19.499	2
361	1.9900	30.017	16.378	1
362	1.4730	4.152	17.546	1
363	0.4190	21.120	19.737	1
364	0.2230	24.818	18.708	1
365	0.5820	1.253	19.238	1
367	0.0166	5.789	19.487	2
368	1.7330	4.157	14.766	1
369	0.2270	23.414	20.242	1
370	0.4510	32.244	20.039	1
371	0.1280	78.058	19.044	1
372	1.3190	12.852	13.819	1
373	0.4040	7.064	18.977	1
374	1.3670	40.375	15.980	1
376	1.7870	17.612	17.786	1
378	0.3250	14.065	15.811	1
379	0.0996	21.398	18.058	2
381	0.0394	56.161	21.651	2
382	0.1290	19.246	20.478	1
383	0.1030	26.611	18.358	1
384	0.0625	16.452	20.484	2
385	1.5030	11.916	16.891	1
386	1.0400	46.342	18.149	1
387	1.8590	10.853	17.293	1
388	0.1790	5.950	20.196	1
389	1.8930	60.328	16.388	1
390	0.3010	25.100	19.210	1
391	1.3410	26.816	17.490	1

Table 2—Continued

OGLE ID Number	u_0	t_E (days)	$I(source)$ (mag)	Code ^a
392	0.0900	14.409	19.580	1
393	0.0360	25.254	18.996	1
394	0.3280	22.852	16.218	1
396	0.4380	21.745	18.573	1
397	0.1440	6.435	17.893	1
398	1.8040	19.059	17.302	1
399	1.7080	5.376	17.291	1
400	0.7430	15.860	18.922	1
401	0.9940	2.374	18.675	1
402	0.1030	22.956	20.509	1
403	0.8820	3.038	18.452	1
404	0.4720	47.022	17.707	1
405	1.0190	7.443	18.516	1
406	0.4430	135.727	17.821	1
407	0.2130	14.191	19.496	1
408	0.0970	70.366	21.145	1
409	0.1278	8.463	19.314	2
411	1.1170	10.462	18.160	1
412	0.2730	12.754	18.587	1
413	0.0420	71.227	19.946	1
414	0.3370	19.779	19.807	1
415	0.9630	7.086	18.541	1
416	0.1750	13.885	19.731	1
417	0.5380	30.552	17.669	1
418	1.0750	26.804	18.484	1
419	0.5170	1.691	19.546	1
420	1.2970	0.862	16.374	1
422	0.0940	51.855	19.534	1
424	0.7050	2.990	18.748	1
425	0.0651	13.534	20.034	2

Table 2—Continued

OGLE ID Number	u_0	t_E (days)	$I(source)$ (mag)	Code ^a
427	0.1170	17.079	20.070	1
428	0.9990	20.815	17.593	1
429	1.5810	19.908	17.914	1
430	0.6040	5.960	19.479	1
431	0.1260	6.614	20.526	1
432	0.1830	12.875	20.486	1
433	0.3050	140.296	19.289	1
434	0.0470	16.235	19.382	1
435	0.2160	4.306	19.657	1
436	0.5980	6.403	19.272	1
437	1.3650	11.424	18.252	1
438	0.6880	9.784	19.104	1
439	0.3880	14.374	16.165	1
440	0.0270	25.729	22.025	1
441	0.5410	24.898	17.742	1
442	0.8100	35.378	15.994	1
443	0.3540	2.921	19.102	1
444	0.2610	11.301	19.845	1
445	1.6250	2.028	15.874	1
446	0.2400	39.482	19.356	1
447	0.2240	26.307	18.974	1
448	0.0130	7.294	20.117	2
450	0.9740	0.942	17.024	1
451	0.3410	28.792	19.658	1
452	0.2020	24.725	19.998	1
453	0.0840	9.360	18.521	1
454	1.3520	3.883	17.602	1
455	0.9590	38.684	18.833	1
457	0.6280	23.806	18.542	1
458	0.1890	13.473	18.837	1

Table 2—Continued

OGLE ID Number	u_0	t_E (days)	$I(source)$ (mag)	Code ^a
459	0.2570	10.406	15.693	1
460	0.5600	8.696	16.219	1
461	0.7200	9.363	18.908	1
462	0.2270	27.770	18.824	1
463	0.2480	128.839	20.576	1
464	0.2640	7.622	19.199	1
465	1.0840	16.685	18.668	1
467	0.6900	39.481	19.354	1
468	0.5600	10.284	19.198	1
469	0.5910	9.910	19.029	1
470	0.2520	27.651	20.155	1
472	0.1730	9.497	20.063	1
473	1.6690	3.063	15.282	1
474	0.8360	33.763	19.083	1
475	0.1110	16.064	20.139	1
477	0.4500	11.825	18.931	1
478	0.2430	27.199	16.950	1
479	0.3818	0.364	17.172	2
480	0.1090	32.168	20.672	1
481	1.2000	6.392	18.085	1
482	0.5490	19.748	19.266	1
483	0.1200	108.671	19.948	1
484	0.6400	77.937	19.389	1
485	0.5290	36.986	16.370	1
486	0.2720	18.947	19.858	1
487	1.0100	9.668	18.666	1
488	0.3060	42.792	18.618	1
490	0.9790	15.707	18.674	1
491	0.6370	30.693	16.573	1
492	0.5590	6.773	19.181	1

Table 2—Continued

OGLE ID Number	u_0	t_E (days)	$I(\text{source})$ (mag)	Code ^a
494	0.9420	17.071	18.438	1
496	0.4000	16.050	20.085	1
497	0.7540	8.634	18.940	1
498	0.1720	4.420	19.054	1
499	0.5060	30.736	18.584	1
500	0.5290	28.069	19.398	1
502	0.7810	24.971	18.943	1
503	0.8080	5.603	14.719	1
504	1.1120	4.145	15.964	1
505	1.4830	17.909	16.925	1
507	0.4590	8.735	17.914	1
508	1.2910	3.361	17.270	1
509	0.0634	6.060	16.541	2
510	0.0600	21.642	19.211	1
512	0.1650	13.080	19.310	1
515	0.1240	28.342	20.778	1
517	1.0020	18.985	15.190	1
519	1.0210	19.208	18.040	1
520	0.0710	113.894	20.778	1
521	0.3680	10.199	19.135	1
523	0.8350	1.020	17.654	1
525	0.2970	13.054	17.243	1
526	0.1930	35.549	19.610	1
528	0.3950	14.820	18.551	1
529	0.5700	8.373	18.966	1
531	0.7760	35.459	18.594	1
532	0.8580	2.815	17.516	1
533	0.2580	6.458	19.620	1
534	0.8760	77.565	17.637	1
536	1.0380	1.942	16.819	1

Table 2—Continued

OGLE ID Number	u_0	t_E (days)	$I(source)$ (mag)	Code ^a
537	0.7110	4.836	17.760	1
538	0.9990	35.077	18.821	1
539	0.4690	12.476	17.121	1
542	0.4880	32.895	19.134	1
543	0.0414	8.027	20.189	2
544	0.3240	51.769	17.781	1
546	0.2780	7.082	20.024	1
548	1.1940	1.326	17.926	1
550	0.6340	4.005	18.042	1
551	0.3140	87.720	19.684	1
552	0.2550	9.258	19.412	1
553	0.2720	16.275	19.630	1
554	0.7960	8.127	18.478	1
555	0.1633	4.431	17.312	2
556	0.0170	6.049	20.086	2
558	1.6880	5.801	15.644	1
560	0.5630	10.134	18.858	1
562	1.0800	20.369	18.143	1
563	1.0800	13.784	18.143	1
564	0.0154	48.033	20.759	2
565	0.5210	35.009	19.134	1
566	0.4180	13.212	20.080	1
568	0.1750	17.327	20.728	1
569	0.5310	6.221	19.187	1
571	1.5310	5.951	16.070	1
572	0.6500	21.002	19.597	1
573	0.1600	20.472	19.380	1
574	0.4760	21.279	16.261	1
575	1.0260	5.529	17.790	1
577	1.0880	19.076	17.110	1

Table 2—Continued

OGLE ID Number	u_0	t_E (days)	$I(source)$ (mag)	Code ^a
579	1.3100	3.176	16.621	1
580	0.1610	12.775	18.580	1
582	0.6130	34.789	14.121	1
583	0.7820	19.729	17.293	1
585	1.8410	9.477	16.402	1
587	0.3450	8.151	19.522	1
589	0.4140	2.645	17.648	1
590	1.0020	4.988	17.476	1
591	0.5980	19.129	18.390	1
593	0.9480	3.298	15.812	1
595	0.9200	21.426	16.049	1
596	0.1150	9.811	19.672	2
597	0.3480	16.634	19.444	1
598	1.3320	5.988	16.158	1
599	0.8280	8.373	15.552	1
600	0.5570	30.395	16.637	1
601	0.1390	22.435	14.648	1
602	1.0050	18.815	17.858	1
604	0.3270	22.569	18.901	1
605	1.5360	14.926	16.404	1
607	0.3830	11.086	19.914	1
608	0.0073	17.533	21.042	2
609	0.8290	24.632	18.557	1
610	0.0251	0.172	21.514	2
611	1.0930	4.195	17.058	1
612	0.1750	13.667	20.034	1
614	0.4640	11.229	19.074	1
615	0.0207	94.549	22.290	2
616	0.1880	12.036	16.891	1
617	1.1900	18.426	14.581	1

Table 2—Continued

OGLE ID Number	u_0	t_E (days)	$I(source)$ (mag)	Code ^a
618	0.1190	32.709	19.533	1
619	0.1530	10.256	18.821	1
620	0.0260	16.276	21.107	2
621	0.5610	6.337	16.530	1
622	0.0400	56.507	21.010	1
623	0.2950	10.212	19.571	1
624	0.8640	13.415	14.528	1
626	1.1380	24.520	16.455	1
627	0.2100	6.957	19.255	1
630	0.5320	8.272	19.031	1
631	0.0172	76.610	19.838	2
632	0.2200	49.643	19.713	1
634	0.0810	46.988	20.907	1
635	0.2420	15.499	17.635	1
636	0.0370	11.119	17.964	1
637	0.6670	4.239	18.118	1
638	0.0000	85.649	20.414	2
639	1.3130	10.793	17.478	1
640	0.9740	5.510	17.173	1
641	0.8110	6.714	14.634	1
644	0.2530	46.765	18.432	1
645	0.6290	25.406	18.706	1
646	0.0426	23.954	19.293	2
647	0.1020	91.987	20.506	1
651	0.2740	9.882	17.279	1
653	0.3970	36.205	17.838	1

^a1 = original values unchanged, 2 = altered. Events for which u_0 could not be reliably determined or estimated are not listed.